

Element-specific magnetic hysteresis as a means for studying heteromagnetic multilayers

C. T. Chen

AT&T Bell Laboratories, 600 Mountain Avenue, Murray Hill, New Jersey 07974

Y. U. Idzerda

Naval Research Laboratory, Washington, D.C. 20375

H.-J. Lin and G. Meigs

AT&T Bell Laboratories, 600 Mountain Avenue, Murray Hill, New Jersey 07974

A. Chaiken* and G. A. Prinz

Naval Research Laboratory, Washington, D.C. 20375

G. H. Ho

Department of Physics, University of Pennsylvania, Philadelphia, Pennsylvania 19104

(Received 9 April 1993)

We report element-specific magnetic hysteresis measurements on heteromagnetic materials. Dramatically different Fe and Co hysteresis curves of Fe/Cu/Co trilayers were obtained by recording the magnetic circular dichroism at their respective L_3 white lines as a function of applied magnetic field. The data resolve the complicated hysteresis curves, observed by conventional magnetometry, and determine the individual magnetic moments for the Fe and Co layers. Fine hysteresis features, imperceptible in the conventional curves, were also observed, demonstrating a new and powerful means for studying heteromagnetic multilayer systems.

The most fundamental characterization of a magnetic material is its magnetization as a function of applied field. This yields not only the magnetic moment, but also provides valuable information on the magnetic anisotropy and coupling between the magnetic elements of the material. From the hysteresis of the measurement, one can extract important secondary properties, such as the coercive field and the remnant magnetization, which depend upon details of domain formation and reversal.¹ Until now, all magnetic hysteresis curves have been obtained by techniques which probe the overall magnetic behavior of the sample, such as in various magnetometries,¹ magneto-optical Kerr effect,²⁻⁴ and spin-polarized photoemission^{5,6} measurements. For magnetic systems containing more than one magnetically active element, i.e., heteromagnetic systems, element-specific magnetic hysteresis measurements should provide novel information that is unobtainable by these conventional hysteresis measurements. Recent developments in core-level magnetic circular dichroism (MCD), using circularly polarized synchrotron radiation, have made it rather easy to investigate the magnetic properties of matter with element and site specificities.⁷⁻¹³ Considering the large absorption cross section and the strong MCD effect observed at the $L_{2,3}$ white lines of $3d$ transition metals and at the $M_{4,5}$ white lines of $4f$ rare-earth elements^{8,10-13} one would expect to be able to measure element-specific magnetic hysteresis curves using soft-x-ray MCD.

In this paper, we report element-specific magnetic hysteresis measurements on heteromagnetic materials. By recording the L_3 MCD signal as a function of applied magnetic field, dramatically different hysteresis curves for the Fe and Co layers were obtained from the Fe/Cu/Co trilayer system. The complicated conventional hysteresis curves, obtained with a vibrating sample magnetometer,

were resolved as a linear combination of the two elemental hysteresis curves, thereby determining the magnetic moments for the Fe and Co layers. Fine features were also observed in the Co hysteresis curves, providing new information on the magnetic interactions in this trilayer system. This work demonstrates that element-specific magnetic hysteresis measurements are now feasible and serve as a powerful means for studying heteromagnetic materials.

The measurements were conducted at the AT&T Bell Laboratories Dragon beamline at the National Synchrotron Light Source.¹⁴ The monochromator set up for soft-x-ray magnetic circular dichroism measurements has been described previously.^{8,14} The photon energy resolution was set at 0.4 eV, and the degree of circular polarization was set at 77% to optimize the circular dichroism signal-to-noise ratio.¹⁴ The hysteresis measurements were performed using a compact, liquid-nitrogen-cooled, UHV compatible electromagnet which can be scanned using a computer-controlled bipolar current power supply. For these measurements, the magnetic field was parallel to the sample surface as depicted in Fig. 1. The angle of the incident beam (labeled as $h\nu$ in Fig. 1) is fixed at 45° with respect to the surface normal, and the absorption spectra were recorded by monitoring the soft-x-ray fluorescence yield (labeled as $h\nu'$ in Fig. 1) with a high sensitivity seven-element germanium detector. The use of the fluorescence yield method is essential for measuring the MCD spectra in an applied field and, because of its large probing depth, ~ 1000 Å, allows the investigation of buried layers.

To demonstrate the essential features of element-specific magnetic hysteresis measurements, two Fe/Cu/Co trilayer structures were grown by evaporation onto glass substrates held at elevated temperatures.

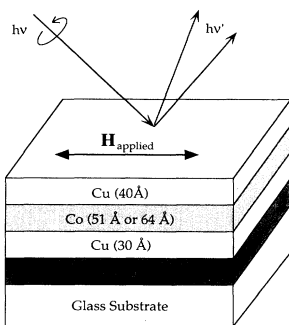


FIG. 1. Geometric arrangement for element-specific magnetic hysteresis measurements. $h\nu$, $h\nu'$, and H_{applied} stand for incident circularly polarized soft-x-ray beam, soft-x-ray fluorescence yield, and the applied magnetic field, respectively.

The elemental atomic concentrations present in the two trilayer films were determined by hard-x-ray fluorescence to correspond to a film thickness of Fe(102 Å)/Cu(30 Å)/Co(51 Å), to be referred to as the *thick* Fe/Cu/Co trilayer sample, and Fe(53 Å)/Cu(30 Å)/Co(64 Å), to be referred to as the *thin* Fe/Cu/Co trilayer sample. Both samples were capped with an additional 40 Å Cu layer to protect them from oxidation.

Figure 2 shows the Fe and Co $L_{2,3}$ normalized-fluorescence-yield soft-x-ray absorption spectra of the thick Fe/Cu/Co trilayer sample. The solid (dashed) lines were taken with the projection of the spin of the incident photons parallel (antiparallel) to the spin direction of the majority 3d electrons. These spectra were measured by alternating between opposite applied saturating magnetic

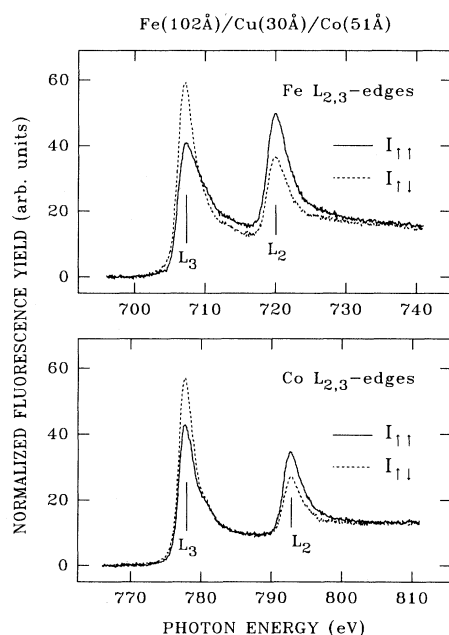


FIG. 2. Fe and Co $L_{2,3}$ edge fluorescence-yield x-ray absorption spectra of the thick Fe/Cu/Co trilayer sample. The solid (dashed) line is taken with the projection of the spin of the incident photons parallel (antiparallel) to the spin of the majority 3d electrons. L_3 and L_2 indicate the $2p_{3/2} \rightarrow 3d$ and $2p_{1/2} \rightarrow 3d$ absorption white lines, respectively.

fields, ± 0.7 KOe, at each photon energy while the circular polarization was held constant. Measurements taken with constant magnetic field and alternating circular polarization, using the two-beam configuration of the Dragon beamline and its fast *in situ* photon chopper,¹⁴ have shown nearly identical spectra. The peaks labeled as L_3 and L_2 in the figures are the $2p_{3/2} \rightarrow 3d$ and $2p_{1/2} \rightarrow 3d$ soft-x-ray absorption white lines. After being normalized by the incident photon beam intensity, the spectra show virtually no MCD effect at photon energies below the L_3 and well above the L_2 white lines. To help quantify the MCD effect of the L_3 white lines, the vertical scales are labeled such that the baseline and the mean value of the two L_3 peak heights are equal to 0 and 50, respectively. In the following discussion, we define MCD and x-ray absorption spectroscopy (XAS) intensities as $(I_{\uparrow\uparrow} - I_{\uparrow\downarrow})$ and $(I_{\uparrow\uparrow} + I_{\uparrow\downarrow})$, respectively, where $I_{\uparrow\uparrow}$ and $I_{\uparrow\downarrow}$ are the measured fluorescence yields for parallel and antiparallel electron-photon spin alignments. Correcting for the incomplete circular polarization (77%) and the incident photon angle (45°), the corrected spectra [a multiplicative factor of $1/(0.77 \times \sin 45^\circ)$] show giant L_3 MCD to XAS peak height ratios of 35% for Fe and 26% for Co.

Currently, there is great interest in deducing fundamental parameters, such as exchange splitting, spin-orbit interaction, and spin and orbital magnetic moments from the MCD and XAS spectra,^{8,12,13,15,16} however, no general procedure has yet been experimentally verified to extract accurate values from these data. We believe that in order to extract reliable absolute quantities for any given sample, absolute absorption cross-section measurements, as well as first-principle calculations which take into account the various electron correlation and band structure effects are necessary. Nevertheless, it has been demonstrated both experimentally⁷⁻¹³ and theoretically¹⁶ that for a given sample the MCD to XAS ratio of the white lines of each element in a given site is proportional to the average magnetic moment (i.e., the magnetic ordering) in that site. Based on this, one would expect to measure element-specific magnetic hysteresis curves by recording the peak height of a given elemental white line as a function of applied magnetic field. The top panel of Fig. 3 shows the results of such measurements taken with the photon energies tuned at the Fe and Co L_3 white lines, respectively. The measured peak heights were plotted relative to their mean value and scaled to span from -1 to $+1$, i.e., $[2I - (I_{\uparrow\uparrow} + I_{\uparrow\downarrow})]/(I_{\uparrow\uparrow} - I_{\uparrow\downarrow})$, where I stands for the measured intensity at a given applied magnetic field. Hysteresis behavior is clearly observed in both curves as expected, but the Fe and Co curves show dramatic differences. While the Fe layer shows a square hysteresis loop with a coercive field of 38 Oe and a saturation field of ~ 100 Oe, the Co layer shows a less abrupt hysteresis loop with a larger coercive field of 201 Oe and a saturation field of ~ 450 Oe. It was found that, regardless of the photon energy chosen, the functional form of the measured hysteresis curves is always nearly identical, as long as there is sufficient MCD signal to measure with. This implies that the *peak height* method gives the same results as the much more tedious and difficult *peak area* method.

Although the Fe hysteresis loop is representative of a single film, the fine structure observed at low field in the Co hysteresis loop clearly demonstrates that the Co film has two distinct components. The onset of this feature corresponds exactly with the switching of the Fe film, demonstrating that the Fe film and a fraction of the Co film are magnetically coupled. The most probable cause of this coupling is that the Cu interlayer is not complete, resulting in direct contact between the Fe and Co films via pinholes through the interlayer Cu film. The strong dipole coupling generated by the intimate contact between the Fe film and a small portion of the Co film results in identical switching fields. A similar behavior for the element-specific hysteresis loops should be expected if a limited interdiffusion between the Fe and Co had occurred. For an interdiffused region, the hysteresis curves of the Fe and Co would be identical, as observed in our measurements of $\text{Fe}_x\text{Co}_{1-x}$ alloy thin films which displayed identical Fe and Co hysteresis curves. Although we cannot completely rule out this possibility, the interdiffusion is unlikely because the temperature required for it to occur is well above the low sample growth temperature (170 °C) used here.

These fine hysteresis features, imperceptible in the vibrating-sample magnetometer (VSM) data but observed in the element-specific measurements have important ramifications for understanding other phenomena involving magnetic heterostructures, particularly the giant magnetoresistance (GMR) effects for which multilayer systems have been used to measure the overall conductivity difference between magnetically aligned and antialigned film structures.^{17–20} For the trilayer illustrated here, we see that a fraction of the Co film is always aligned with the Fe film, thus reducing the measured GMR effect. These element-specific measurements serve as an excellent probe for interfacial coupling and could play an important role in understanding these effects in GMR structures.

To appraise how well the element-specific magnetic hysteresis curve represents the magnetic moment of a given element, the bottom panel of Fig. 3 shows the comparison between the measured conventional hysteresis curve obtained using a vibrating-sample magnetometer (solid line labeled VSM) and its least-square-best-fit linear combination of the Fe and Co hysteresis curves (dashed line labeled as Fe+Co). The fit to the VSM data by the Fe+Co curve can be obtained by multiplying the individual Fe and Co curves of the top panel by the total number of Fe and Co atoms and by their respective elemental magnetic moments, then summing them. If the total number of Fe and Co atoms is known (in this case, experimentally determined by hard-x-ray fluorescence), then the fit determines the elemental magnetic moments. Our best fit determined average magnetic moments of $(2.1 \pm 0.08)\mu_B$ per Fe atom and $(1.2 \pm 0.05)\mu_B$ per Co atom for the thick Fe/Cu/Co sample, giving saturated total moments of 1.72×10^{-3} and 0.51×10^{-3} emu for the Fe and Co layers, respectively. Also shown in the bottom panel are the constituent Fe and Co hysteresis curves of the best fit, obtained by multiplying these total moments by their respective curves shown in the top

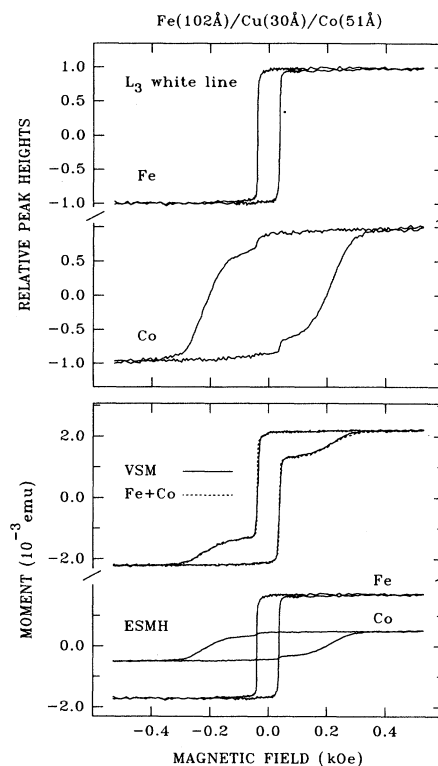


FIG. 3. The top panel shows the Fe and Co L_3 white line intensities as a function of the applied magnetic field for the thick trilayer sample. The bottom panel shows the comparison between the conventional hysteresis curve obtained by a vibrating sample magnetometer (solid line; labeled VSM) and its least-squares-best-fit linear combination of the Fe and Co curves (dashed line; labeled Fe+Co). Also shown in the bottom panel are the constituent Fe and Co element-specific magnetic hysteresis (ESMH) curves of the best fit. The magnetic moment shown here is normalized for a $1 \times 1 \text{ cm}^2$ thin film.

panel. The resulting Fe+Co curve is in excellent agreement with the VSM curve, proving that the abrupt low field region of the VSM curve measures the switching of the Fe layer, and the more gradual transition region measures the switching of the Co layer.

To investigate whether this linear combination procedure is applicable to films of different layer thickness, the top panel of Fig. 4 shows the L_3 peak height measurements of the thin Fe/Cu/Co trilayer sample. Except for some minor but interesting changes, these curves are qualitatively similar to those of the thick sample, a square loop for Fe and a rounded loop for Co. The bottom panel of Fig. 4 shows the comparison between the VSM and its least-squares-best-fit Fe+Co curves. Although there are minor discrepancies between the two curves, the overall agreement is very good. The thin Fe/Cu/Co trilayer sample was found by VSM to exhibit a significant in-plane uniaxial magnetic anisotropy, resulting in a substantial variation in the hysteresis loop with sample azimuthal rotations. These minor discrepancies could be due to a slight misalignment of the in-plane crystalline axis with the applied field direction in the MCD measurements. Our best-fit determined average magnetic mo-

ments of $(2.0 \pm 0.08)\mu_B$ per Fe atom and $(1.1 \pm 0.04)\mu_B$ per Co atom for the thin Fe/Cu/Co sample, giving saturated total moments of 0.85×10^{-3} and 0.57×10^{-3} emu for the Fe and Co layers, respectively. While the Fe moments of $2.1\mu_B$ and $2.0\mu_B$ determined for these two films are close to the bulk Fe moment of $2.2\mu_B$, the Co moments of $1.2\mu_B$ and $1.1\mu_B$ are reduced from the bulk Co moment of $1.7\mu_B$. A similar reduction for the measured Co moment for Co/Cu superlattices has recently been reported, in which the Co moment was determined to be $1.3\mu_B - 1.4\mu_B$.²¹

We emphasize that the linear combination procedure presented above does not require absolute MCD or XAS measurements. Only the functional form of each individual hysteresis curve is needed. For heterostructures which have more than one layer containing identical elements, e.g., the Fe/Cr/Fe trilayer system, one could still obtain the functional form of the hysteresis curve of each layer by measuring the MCD of different magnetic trace elements intentionally doped into different layers, e.g., Ni for one Fe layer and Mn for the other. The trace element should display a hysteresis functional form identical to its parent layer, as demonstrated by our measurements of Fe_xCo_{1-x} alloys. In addition, these trace elements can be selectively placed in different regions of the film (e.g., near an interface, at the film center, near the surface) to monitor the variation of the magnetic direction and moment with position within the film.

In conclusion, we have demonstrated the feasibility of element-specific magnetic hysteresis measurements on heteromagnetic materials. Fe and Co individual hysteresis curves of Fe/Cu/Co trilayers were obtained, using the soft-x-ray magnetic circular dichroism technique. A linear combination procedure has been presented to resolve the complicated conventional hysteresis curve and to determine the average magnetic moment for each individual element. Fine hysteresis features, imperceptible in conventional measurements, were observed, providing fingerprints of possible interlayer magnetic interactions in this trilayer system. This new technique of

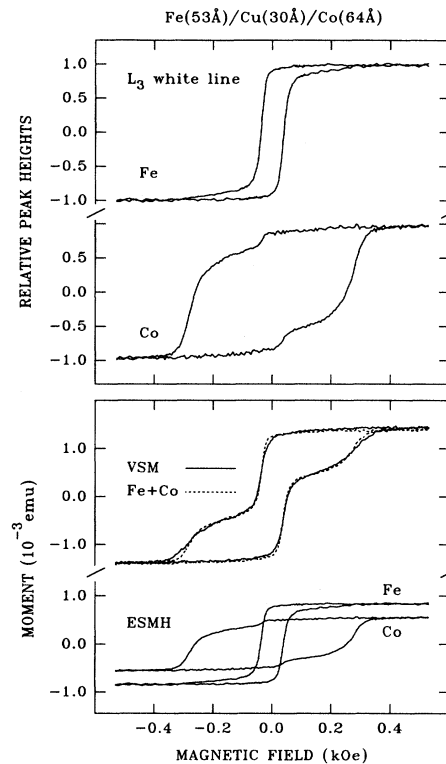


FIG. 4. Element-specific and conventional magnetic hysteresis curves of the thin Fe/Cu/Co trilayer sample. The description for this figure is the same as that of Fig. 3.

element-specific magnetic hysteresis measurements provides a powerful means for studying heteromagnetic materials, particularly for multilayer systems.

We would like to thank E. Chaban for his excellent technical assistance. Work done at National Synchrotron Light Source was supported by DOE, under Contract No. DE-AC02-76CH00016.

*Present address: Condensed Matter and Analytical Sciences Division, Lawrence Livermore National Laboratory, Livermore, CA 94551.

¹See, for example, S. Chikazumi, *Physics of Magnetism* (Kreiger, Boca Raton, FL, 1986).

²Z. Q. Qiu, J. Pearson, and S. D. Bader, *Phys. Rev. Lett.* **67**, 1646 (1991).

³W. R. Bennett, W. Schwarzacher, and W. F. Egelhoff, Jr., *Phys. Rev. Lett.* **65**, 3169 (1990).

⁴G. A. Mulhollan, R. L. Fink, and J. L. Erskine, *Phys. Rev. B* **44**, 2393 (1991).

⁵M. Campagna *et al.*, *Adv. Electron. Electron Phys.* **41**, 113 (1976).

⁶M. Stampanoni *et al.*, *Phys. Rev. Lett.* **59**, 2483 (1987).

⁷G. Schütz *et al.*, *Phys. Rev. Lett.* **58**, 737 (1987).

⁸C. T. Chen *et al.*, *Phys. Rev. B* **42**, 7262 (1990).

⁹T. Koide *et al.*, *Phys. Rev. B* **44**, 4697 (1991).

¹⁰P. Rudolf *et al.*, *J. Magn. Magn. Mater.* **109**, 109 (1992).

¹¹L. H. Tjeng *et al.*, *J. Magn. Magn. Mater.* **109**, 288 (1992).

¹²J. G. Tobin, G. D. Waddill, and D. F. Pappas, *Phys. Rev. Lett.* **68**, 3642 (1992).

¹³Y. Wu *et al.*, *Phys. Rev. Lett.* **69**, 2307 (1992).

¹⁴C. T. Chen, *Nucl. Instrum. Methods Phys. Res. Sec. A* **256**, 595 (1987); C. T. Chen and F. Sette, *Rev. Sci. Instrum.* **60**, 1616 (1989); C. T. Chen, *ibid.* **63**, 1229 (1992).

¹⁵C. T. Chen, N. V. Smith, and F. Sette, *Phys. Rev. B* **43**, 6785 (1991); N. V. Smith *et al.*, *ibid.* **46**, 1023 (1992).

¹⁶B. T. Thole *et al.*, *Phys. Rev. Lett.* **68**, 1943 (1992).

¹⁷M. N. Baibich *et al.*, *Phys. Rev. Lett.* **61**, 2472 (1988).

¹⁸P. Levy *et al.*, *J. Appl. Phys.* **67**, 5914 (1990).

¹⁹J. J. Krebs *et al.*, *Phys. Rev. Lett.* **63**, 1645 (1989).

²⁰M. Johnson, *Phys. Rev. Lett.* **67**, 3594 (1991).

²¹C. H. Lee *et al.*, *Phys. Rev. B* **42**, 1066 (1990).